Supporting Information

CO_2 bubbling-based 'Nanobomb' System for Targetedly Suppressing Panc-1 Pancreatic Tumor *via* Low Intensity Ultrasound-activated Inertial Cavitation

Kun Zhang, Huixiong Xu , Hangrong Chen, Xiaoqing Jia, Shuguang Zheng, Xiaojun Cai, Ronghui Wang, Juan Mou, Yuanyi Zheng,* and Jianlin Shi**

Materials

Tetraethoxysilane (TEOS,A.R), Ammonia solution ($NH_3 \cdot H_2O$) (25~28%, A.R) and sodium carbonate anhydrous (Na_2CO_3,A.R) were obtained from Shanghai Lingfeng Chemical Reagent Co.LTD. Methanol (A.R) was purchased from Sinopharm Chemical Reagent Co.,Ltd. Ethyl alcohol absolute (EtOH) was obtained from Shanghai Zhenxing No.1 Chemical Plant. L-arginine (LA) and Cetyltrimethyl Ammonium Bromide (CTAB) was purchased from Sigma-Aldrich. Deionized water was used in all experiments.

Synthesis of S1-S8

In brief, 35.7 ml of ethanol, 5 ml of deionized water, and 1.57 ml of ammonia solution were gently stirred at 30 °C for 30 min. After that, 3 ml pre-warmed TEOS at 30 ºC was injected quickly into above solution and continued stirring for 1 h. After that, white colloidal cores (s-SiO_2) were collected and washed with EtOH and deionized water for twice and once, respectively. The cores were dispersed into 14 ml deionized water by ultrasonication, and then, 2 ml of core dispersion was taken out and diluted with 8 ml deionized water into 10 ml. Next, the 10 ml dispersion was dropwise added into the a solution containing 15 ml EtOH, 15 ml deionized water, 75 mg CTAB and 0.275 ml ammonia solution, and stirred for 30 min. After that, 0.130 ml TEOS was dropwise added into above dispersion, and stirred for another 3 h, forming the S1. Finally, the S1 was collected by centrifugation, and then was etched under different etching conditions for obtaining S2-S8. Detailedly, S2: 15 ml Na_2CO_3 aqueous solution (0.2 M) for 10 h at 50 °C; S3: 15 ml Na_2CO_3 aqueous solution (0.3 M) for 10 h at 50 °C; S4: 20 ml Na_2CO_3 aqueous solution (0.4 M) for 10 h at 50 °C; S5: 20 ml Na_2CO_3 aqueous solution (0.4 M) for 10 h at 60 °C; S6: 20 ml Na_2CO_3 aqueous solution (0.4 M) for 15 h at 60 °C; S7: 20 ml Na_2CO_3 aqueous solution (0.4 M) for 10 h at 70 °C; S8: 20 ml Na_2CO_3 aqueous solution (0.4 M) for 15 h at 70 °C. After further centrifugation, ultrasonication and washing with deionized water and ethanol for several times, the CTAB in as-obtained S1-S8 was removed by extraction with EtOH containing 10% HCl for 24 h per

time and 3 times in sum. The CTAB-extracted S1-S8 samples were dried under vacuum for use.

Synthesis of HMSN-LA

Firstly, 4 g L-arginine was dissolved in 40 ml deionized water *via* magnetic stirring, and after completely dissolution, 400 mg HMSNs (S6) were added and stirred at room temperature for 24 h for adsorbing LA molecules, generating HMSN-LA. After centrifugation, the bottom HMSN-LA was collected and dried *via* vacuum freeze-drying for use, and the unloaded LA molecules in the supernatant were discarded.

Synthesis of HMSN-LA-CO_2 and *in vitro* tests of CO_2 release and LA release

50 mg above-mentioned HMSN-LA was dispersed in 50 ml deionized water, and placed in a special container that allowed the CO_2 gas fluid in, and after reaction for 2 h, the HMSN-LA-CO_2 was collected *via* centrifugation. Two pathways were carried out according to different requirements: (1) to investigate their temperature or pH release behaviors, the harvested samples dispersed in 40 ml degassed water were placed in 100 ml, three-necked, round-bottomed flask with one neck linked to the carrier gas path (N_2) of GC-MS at a total flow rate of 50 $ml \cdot min^{-1}$, and with the 2nd neck linked to the input passage of GC-MS analysis device and with the last one sealed by glass plug, wherein the flask was placed in a oil bath with magnetic stirring for tuning different temperatures and acetic acid was employed to adjust the pH value; (2) to evaluate *in vitro* and *in vivo* capability of killing panc-1 cells, the collected HMSN-LA-CO_2 was re-dispersed in 1640 culture media and stored for use at 4 °C.

As for the release measurement of LA from HMSN-LA-CO_2, 5 mg HMSN-LA-CO_2 sample was loaded in dialysis bag (cutoff MW=3500), and then the bag was placed in 20 ml simulated taken out for UV-Vis measurement, the peak intensity at 205 nm was recorded. Ultimately, according to the concentration-dependent UV-vis standard intensity curve, the release percentage at different time points can be calculated, and release profiles of LA molecules at different pH values could be obtained.

Optical observations of CO_2 bubbles

HMSN-LA or HMSN-LA-CO_2 dispersion in degassed or CO_2 supersaturation solution, and 200 μl dispersion was placed in special 1.5 mm thickness dishes, and coverslip was employed to cover the dispersion, then the whole dish was observed under optical microscope, and hot water can be employed to heat the sealed sample dispersion to generate CO_2 bubbles.

Cell Culture

Panc-1 cells were cultured and maintained in 1640 culture medium with 10% fetal bovine serum at 37 ºC in a fully humidified atmosphere of 5% CO_2.

Cell viability treated with different groups, such as control, US, HMSN-LA, HMSN-LA-CO_2 and US+HMSN-LA-CO_2 *via* MTT method, flow cytometry, confocal observation after PI & calcein double-staining

There are two groups of ultrasound parameters; one is 1 MHz-0.6 W/cm^2-50%-95 KPa, and another is 1 MHz-1.0 W/cm^2-20%-122 KPa, wherein in 1 MHZ is the frequency, 0.6 W/cm^2 and 1.0 W/cm^2 are power density, 50% and 20% are duty cycles, and 95 KPa and 122 KPa are sound pressure. The irradiation is pulsed, and the duration time of each pulse is 15 s with a interval of 60 s, and the number of cycles is 6. To determine the cytotoxicity of HMSN, HMSN-LA, panc-1 cell lines were seeded in 6-well plate at a density of 5×10^5 cells per well in a 3 ml 1640 culture medium. After letting cells settle for 24 h, cells were treated with above-mentioned groups. Aiming to different characterization methods, the following routes accordingly varied, as stated as follows:

MTT method: Herein, aiming at different purposes, different treatments were carried out, and detailed treatment methods aiming at different purposes can be seen in corresponding figure captions. The purposes include the influences of power density, duty cycle, mass concentrations of as-measured samples (HMSN-LA, HMSN-LA-CO_2), exclusion of pH reduction and temperature elevation on the viabilities of panc-1 cell line, respectively. After the treatments with different groups, another 1.5 h incubation was carried out, and then the

upper floated dead cells were discarded. The treated cells were incubated with the MTT reagent for 4 h (viable cells are capable of metabolizing the MTT reagent, while dead cells are not), and 100 μl of DMSO was added to each well and incubated for 30 min, and the absorbance at 570 nm was read. Noticeably, all the employed mass concentrations of HMSN-LA and HMSN-LA-CO_2 in cytotoxicity evaluations kept the same, namely 0.8 mg/ml. Additionally, cytotoxicity of HMSN-LA with different mass concentration was performed on L929 cell line.

Flow cytometry: the ultrasound parameter is 1 MHz-1.0 W/cm^2-20%-122 KPa, and the concentration of sample (HMSN-LA) is 0.8 mg/ml, and HMSN-LA-CO_2 kept the same particle concentration with HMSN-LA. After the treatments with above-mentioned groups, the floated cells were instantly collected and the adherent cells were also harvested, and then all the cells were integrated together for staining. Next, the collected cells were stained by PI and annexin V-FITC, and then the stained cells were instantly tested *via* flow cytometry.

Confocal observation: after PI & calcein double-staining: the ultrasound parameter is 1 MHz-1.0 W/cm^2-20%-122 KPa, and the concentration of sample (HMSN-LA) is 0.8 mg/ml, and HMSN-LA-CO_2 kept the same particle concentration with HMSN-LA. Instead of 6-well plate, the cells were seeded in special 1.5 mm thickness dishes. After the treatments with above-mentioned groups, the floated cells were instantly collected and the adherent cells were also harvested, and then all the cells were regarded as a whole for staining. Next, the collected cells were stained by PI and calcein, and then the stained cells were observed *via* laser confocal microscopy.

SEM observation of panc-1 cells treated with control, HMSN-LA-CO_2 and US+HMSN-LA-CO_2, respectively.

Ultrasound parameter is 1 MHz-1.0 W/cm^2-20%-122 KPa. firstly, special sheet glasses for 48-well plate were placed at the bottom of each well of 48-well plate, and then the panc-1 cell lines were seeded at a density of 2×10^4 cells per well in a 0.4 ml 1640 culture medium so

that cells could climbed on the sheet glasses. After letting cells settle for 24 h, cells were treated with above-mentioned groups, the concentration of sample (HMSN-LA) is 0.8 mg/ml, and HMSN-LA-CO_2 kept the same particle concentration with HMSN-LA. Subsequently, the glasses where cells grew were taken out and washed several times with PBS. Finally, the cells were fixed within 3 s with 2.5% glutaraldehyde solution at 4 °C for 2 h, and then washed twice in PBS. Alcohol dehydration was followed in 33%, 50%, 60%, 80%, 90% and 100% EtOH for 20 min. Each step was repeated twice. After being lyophilized using lyophilization, each sample was coated with Au, and then was observed according to SEM requirements.

Characterizations

FETEM (field emission transmission electron microscopy) analysis was conducted with a JEM 2100 F electron microscope operated at 200 kV to characterize the mesopores and hollow structure. Nitrogen adsorption–desorption isotherms were measured at 77 K on a Micromeritics Tristar 3000 analyzer. The pore-size distributions were calculated using adsorption isotherm branches by the BJH method. Pore volume and specific surface area were calculated by using BJH and BET methods, respectively. Fourier-transform infrared (FTIR) spectra were recorded on a Nicolet Avatar 370 FT-IR spectrophotometer using KBr pellets. UV–vis absorption spectra were obtained with a Shimadzu UV-3101PC UV–vis absorption spectrophotometer. The diagnostic ultrasound for monitoring generation, lifetime, explosion of CO_2 bubbles both *in vitro* and *in vivo* was conducted on Esaote MyLab™90 with a 4-13 MHz transducer, Philips IU22 with equipped with many imaging modalities, respectively and GE LogiQ E9 system with a 8 MHz transducer. The mean diameter and size distribution of samples was measured by dynamic light scattering on Malvern Nano-ZS90. The generation and explosion of CO_2 bubbles *via* ultrasound irradiations with low power density was supplied by a portable ultrasound therapeutic apparatus (Chattanooga, USA). The device for in vivo temperature measurement is FLIR SC300-Series (FLIR Systems AB, Sweden). SEM

images were obtained on a field-emission JEOL JSM-6700F microscope. CO_2 release rate was recorded by a GC-2060 gas chromatograph equipped with a flame ionization detector. Different cell stages were tested on Flow cytometry of Beckman Coulter,Inc., and confocal observation was conducted on Olympus confocal microscopy.

***In vitro* ultrasound imaging**

The as-synthesized HMSN-LA-CO_2 dispersion of a certain concentration (dispersed in degassed PBS) was placed in a plastic tube of 1cm in diameter, and then the bag was immersed into a cistern full of degassed water whose temperature can be tuned *via* a resistance wire or ultrasound irradiations. The detector of ultrasound imaging instrument was fixed on the position with a 2.8 cm distance from the plastic tube. Since CO_2 bubbles will rise rapidly to the wall of elastic rubber bag, in order to observe the dynamic process of CO_2 bubbles' emergence, a long plastic tube was employed to increase the distance from CO_2 bubbles' emergence to the wall of the plastic tube and highly viscous lipiodol was added to hinder the rapid rise of CO_2 bubbles. The videos on the emergence and explosion of CO_2 bubbles under different conditions can also be recorded.

As for the ultrasound-monitoring explosion of CO_2 bubbles, when all adherent CO_2 bubbles fell out of the walls of container (plastic tube) *via* slightly vibration and evenly distributed, the irradiation was conducted on 1 MHz transducer of 1 cm in diameter under 1.0 W/cm^2-20%. Noticeably, the sound-absorbing panel with a hole of 0.5 cm in diameter was placed between the ultrasound transducer and the plastic tube to focus the ultrasound, and simultaneously, diagnostic ultrasound was employed to monitor the explosion process of CO_2 bubbles. In all *in vitro* experiments, Esaote MyLab™90 with a transducer was employed, and the values of average sound intensity can be obtained from an image processing software, SONOMATH—DICOM.

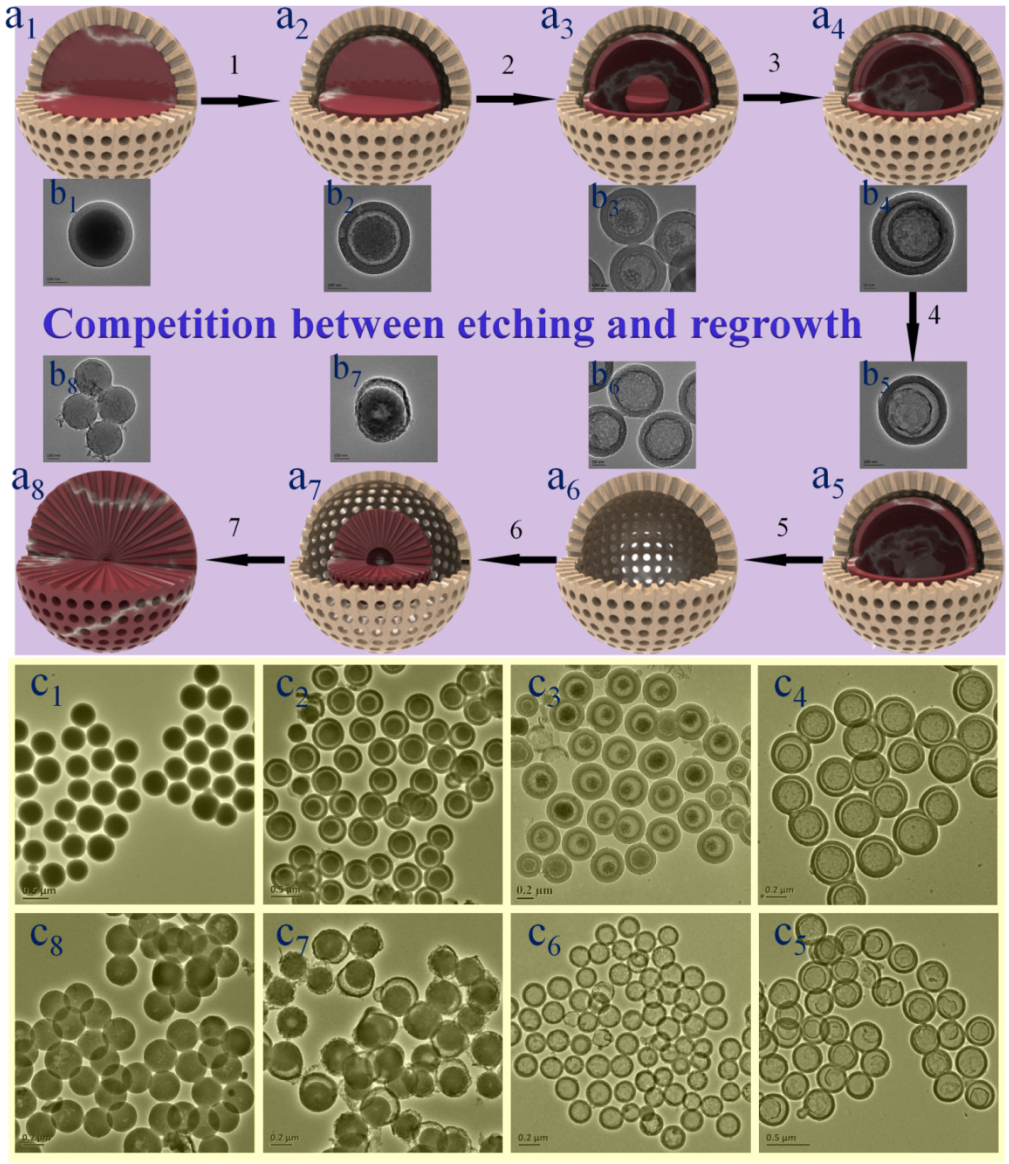

Figure S1 In part A: a_1-h_1) the low-magnification TEM images of different nanostructures respectively corresponding to those from Sample 1 (S1) to Sample 9 (S9) indicated in part B after experiencing different etching phases. a_2-h_2) the high-modification TEM images of S1-S9 obtained after experiencing different etching phases. In part B: Schematic illustrations of the nanostructure evolution process from S1 to S9 in different steps of etching. Detailed descriptions: 1. In the core/shell structure (S1), the interface between inner core and shell was etched away, generating rattle-type structure (S2); 2. In S2, the parts between center and outer surface of inner core was etched away, generating double-shelled rattle-type structure (S3); 3. In S3, inner core was etched out, generating double-shelled hollow mesoporous structure (S4); 4. In S4, the inner shell was further etched away, generating thinner inner shelled double-shelled hollow mesoporous structure (S5); 5. In S5, the inner shell was etched out, generating hollow mesoporous structure (S6); 6. In S6, the outer shell was etched away and were transferred to the inner hollow space, and regenerate outside-in thicker shelled hollow mesoporous silica sphere, forming a thicker inner-shelled double-shelled hollow mesoporous structure (S7); 7. In S7, the outer shell was etched out, and continued being transferred to the thicker inner-shelled hollow mesoporous sphere, and conducted outside-in growth and fill-in the hollow space, forming another mesoporous silica structure (S8).

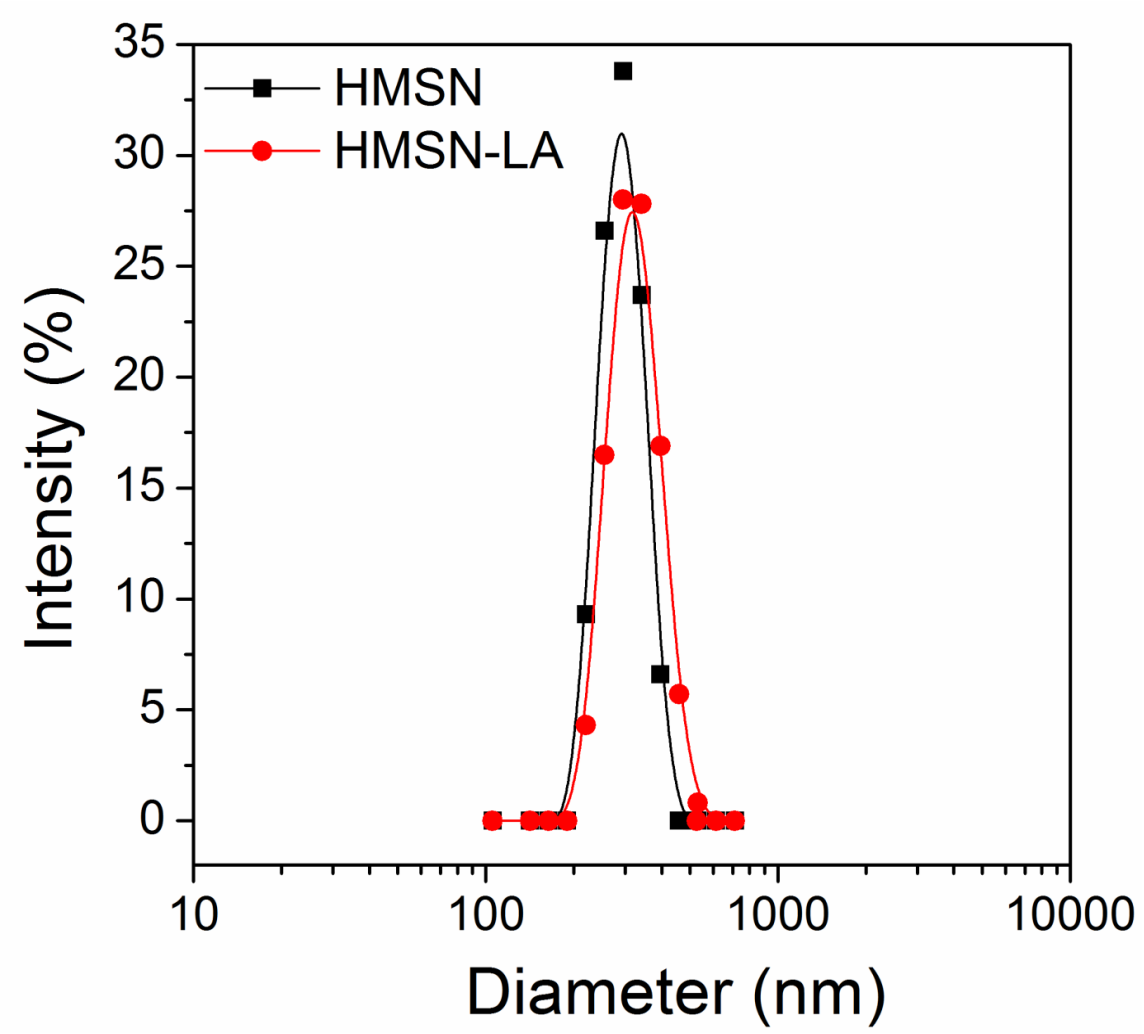

Figure S2 Size distributions of HMSN and HMSN-LA in SBF solution *via* dynamic light scatterin (DLS).

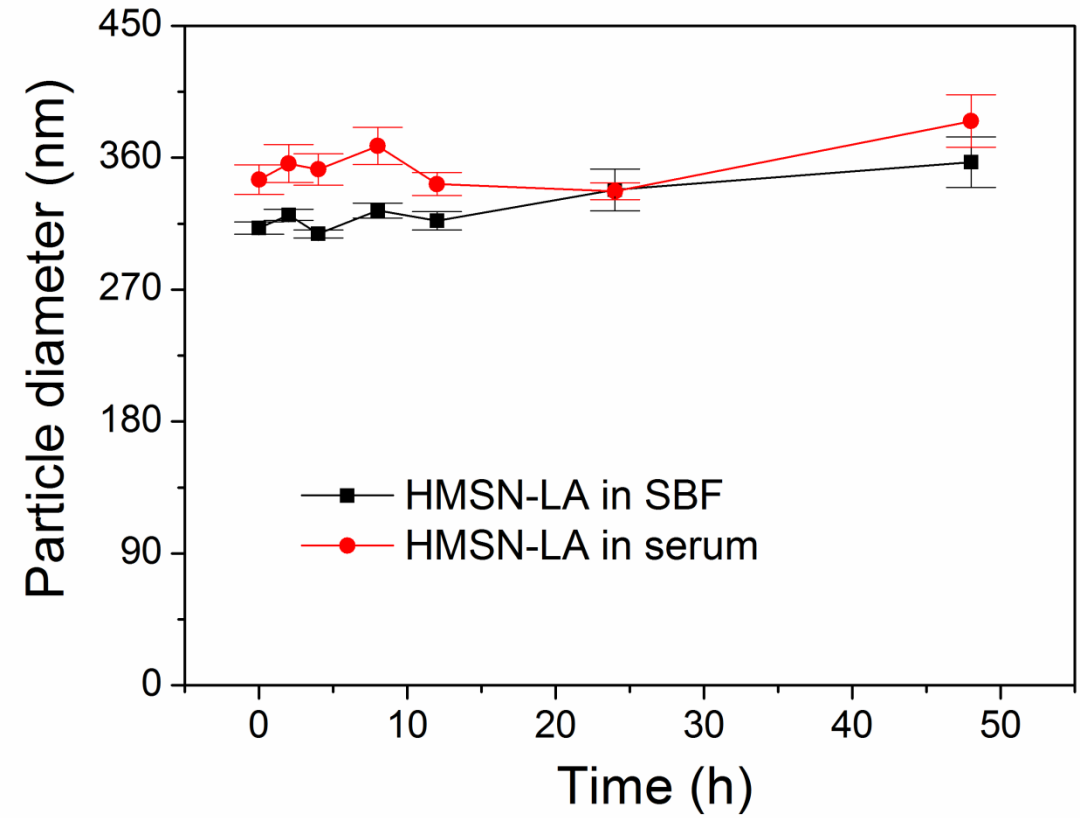

Figure S3 The time-dependent stability evaluations of HMSN-LA in simulated body fluid (SBF) and serum *via* employing DLS to characterizing size variation of HMSN-LA as a function of time.

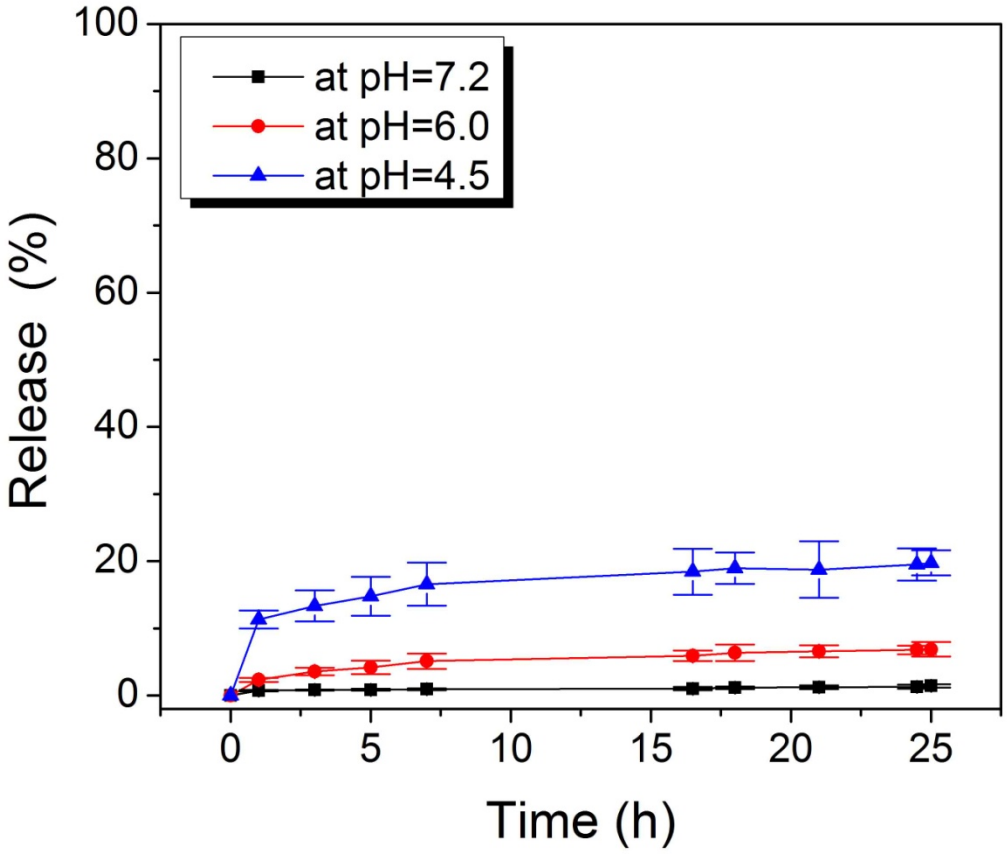

Figure S4. LA release profiles from HMSN-LA-CO_2 at different pH values. Noting: LA was quantitatively measured *via* UV-vis characterization, and according to the standard simulation curve that depicts the relationship between mass concentration of LA molecules and absorbance intensity at 205 nm, the accumulative release amount can be calculated.

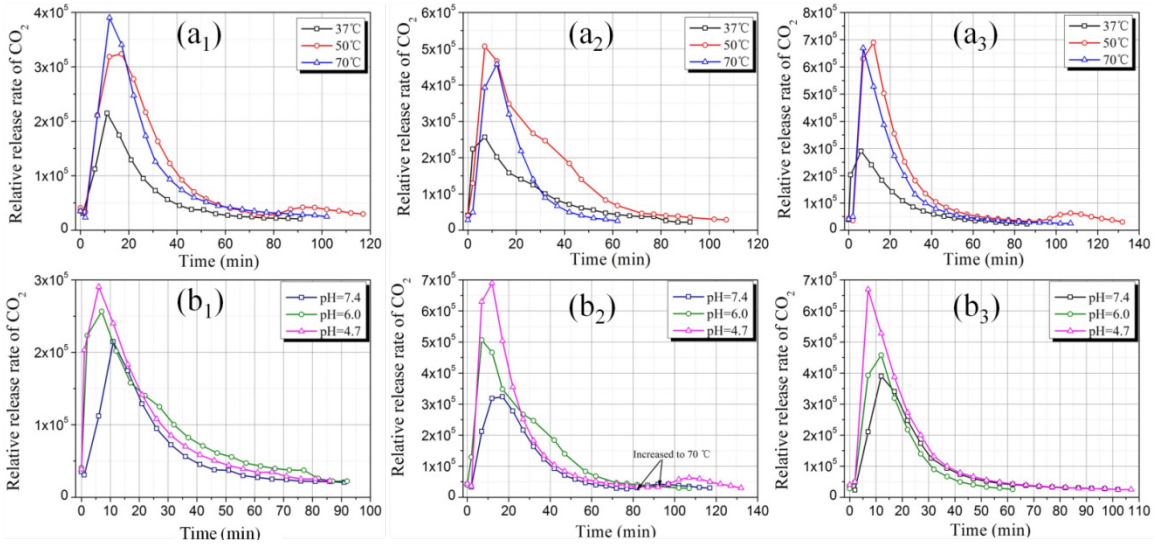

Figure S5 Temperature-dependent relative release rate profiles of CO_2 from HMSN-LA-CO_2 at pH=7.4 (a_1), 6.0 (a_2) and 4.7 (a_3), and pH-dependent relative release rate profiles of CO_2 from HMSN-LA-CO_2 at 37ºC (b_1), 50 °C (b_2) and 70 °C (b_3).

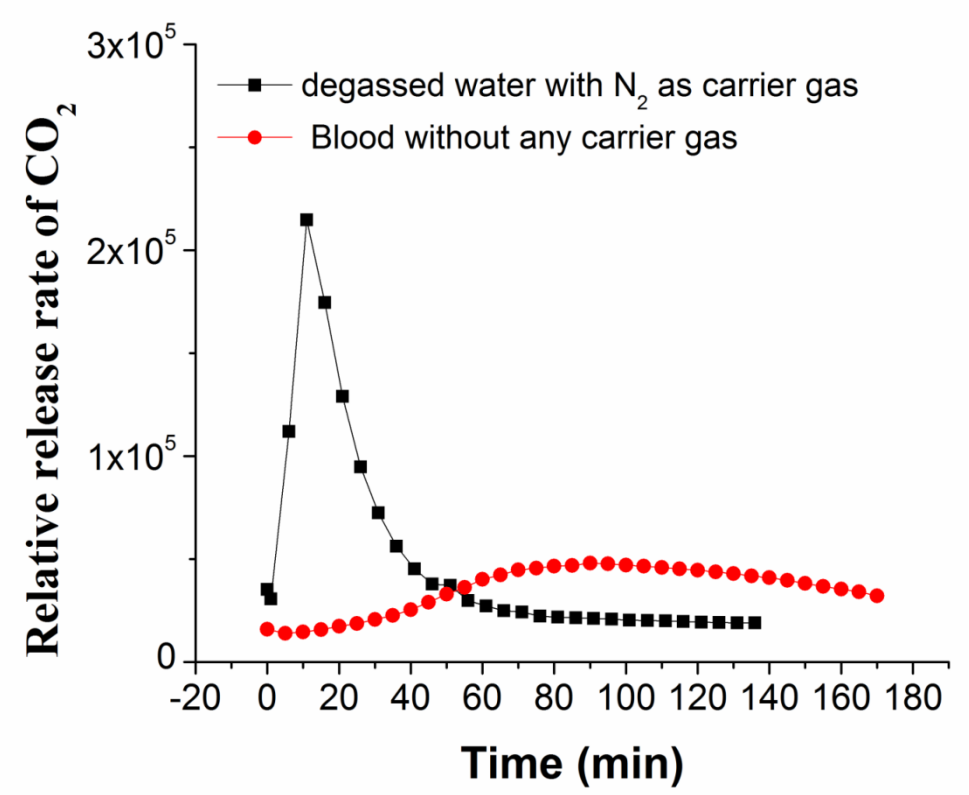

Figure S6. Profiles of relative release rate of CO_2 from HMSN-LA-CO_2 dispersed in degassed water with N_2 as carrier as and blood without any carrier gas.

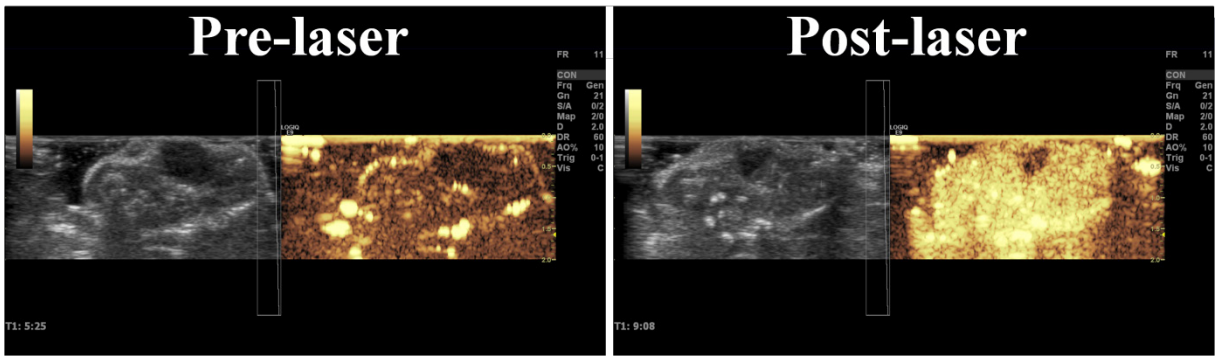

Figure S7 *In vivo* B-mode and contrast-mode ultrasonic images of panc-1 tunors implanted on nude mice. After injecting HMSN-LA-CO_2 samples (0.1 ml, Dose: 10 mg/ml HMSN), 808 nm laser (1.2 W/cm2, 30 s) was employed to heat tumor, and before and after laser irradiation, B-mode and contrast-mode ultrasonic images of tumor were acquired, and MI=0.13 under BFI mode and CHI mode, respectively.

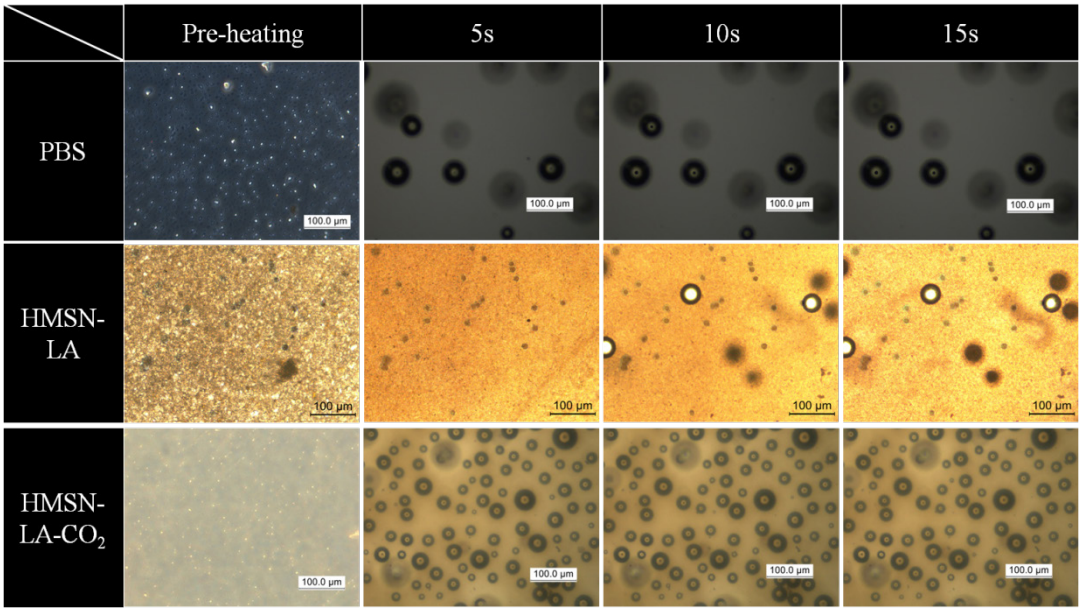

Figure S8 The visual optical microscopic images of PBS, HMSN-LA and HMSN-LA-CO_2 dispersions in degassed PBS before heating (25 °C) and post-heating (50 °C) for 5 s, 10 s and 30 s.

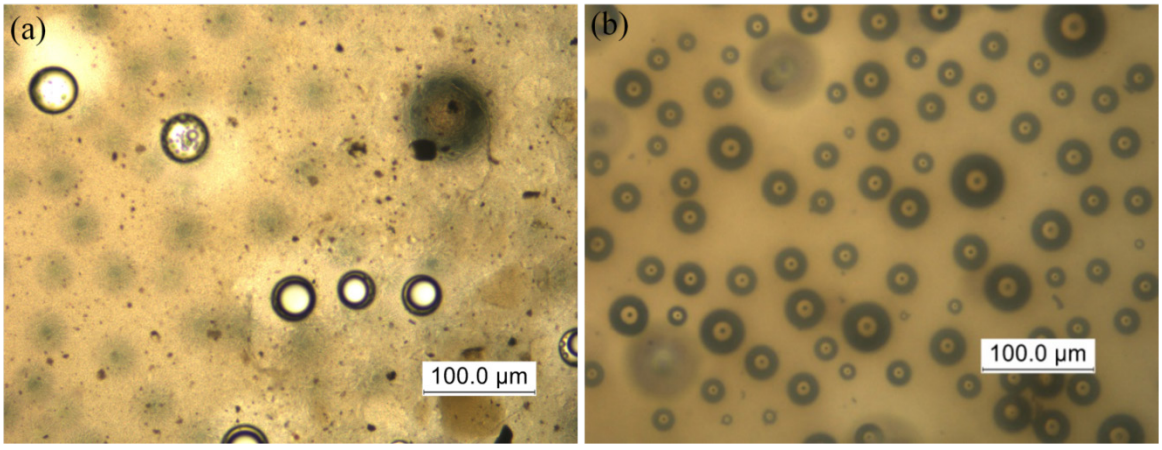

Figure S9 The visual optical microscopic images of HMSN-LA dispersions in CO_2 supersaturated PBS (a) and HMSN-LA-CO_2 dispersion in degassed PBS (b).

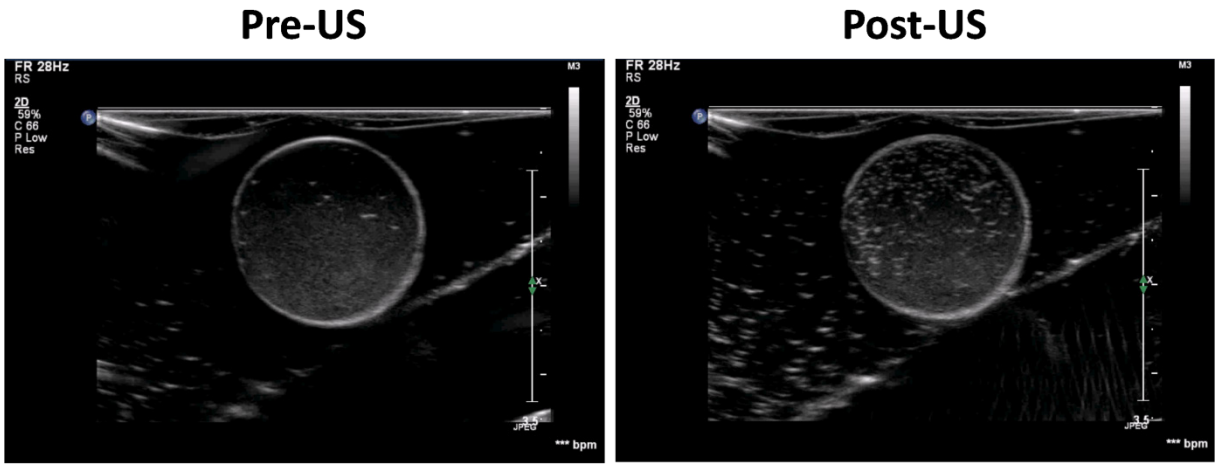

Figure S10. *In vitro* B-mode ultrasonic images of HMSN-LA-CO_2 before and after heating *via* therapeutic ultrasound-mediated hyperpyrexia, and MI=0.6.

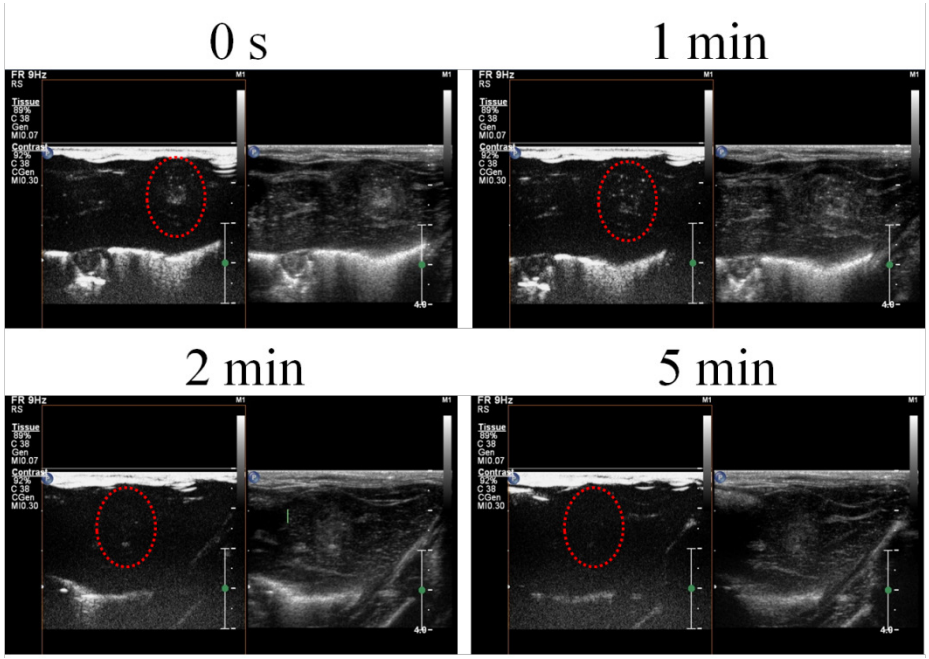

Figure S11 Measurement on CO_2 bubbles' lifetime *in vivo via* ultrasound imaging method. The animal model is VX2 tumor-bearing New Zealand Rabbit, and after intratumorally injecting CO_2 bubbles dispersion received from directly heating HMSN-LA-CO_2 similarly as what video S4 did, ultrasound images at certain timing point were captured, and MI equals to 0.07 and 0.30 under tissue harmonic imagng (THI) mode and CHI mode, respectively.

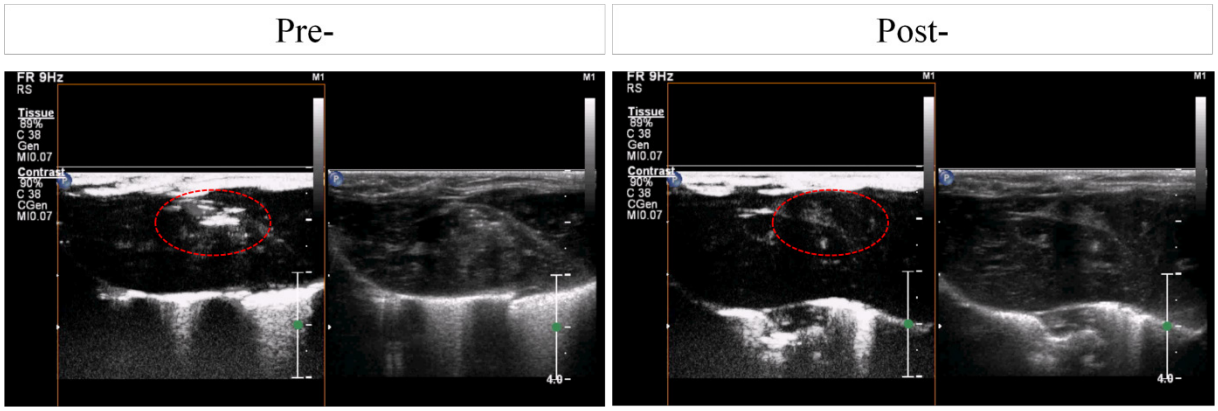

Figure S12 Measurement on *in vivo* ultrasound-triggered explosion of CO_2 bubbles *via* ultrasound imaging method. The animal model is VX2 tumor-bearing New Zealand Rabbit, and after intratumorally injecting CO_2 bubble dispersion which is similar to that in Figure S7, ultrasound irradiations were applied, and ultrasonic images before and after ultrasound irradiations were captured, respectively.Notes: and MI equals to 0.07 under tissue harmonic imagng (THI) mode and CHI mode, respectively

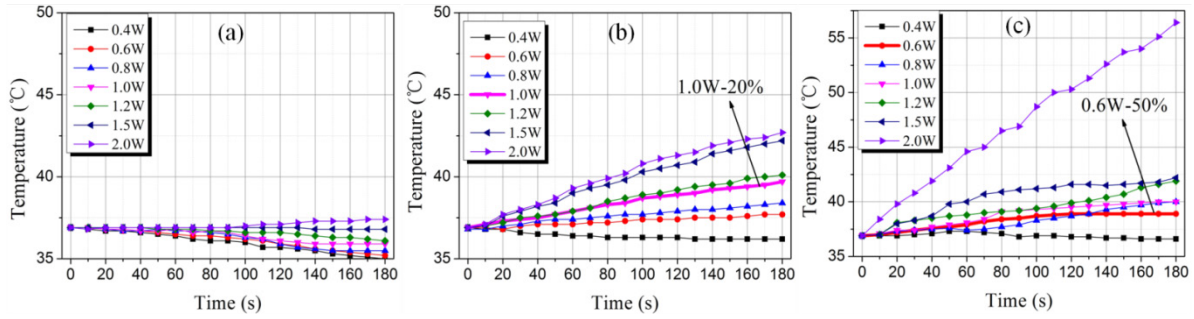

Figure S13 The temperature variations at three different duty cycles: (a) 10%, (b) 20% and (c) 50% when exposure to different power densities, and thermoelectric couple was employed to measure the temperature.

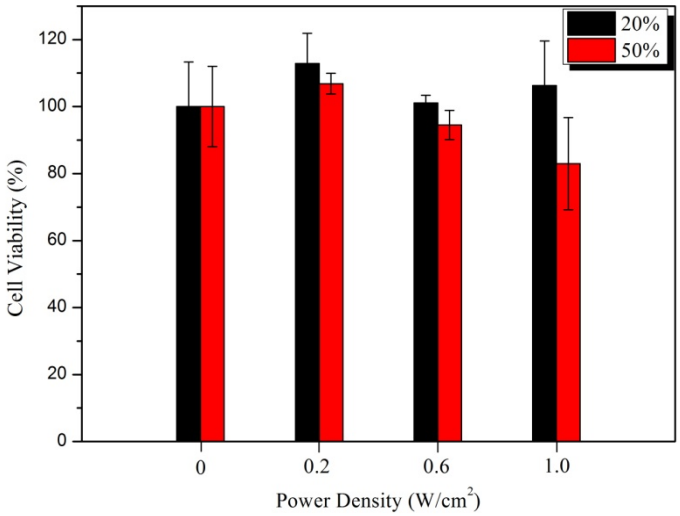

Figure S14 Viability of *in vitro* panc-1 cells treated with different ultrasound groups *via* MTT method for the determination of ultrasound parameters. Other parameters are that ultrasound frequency is 1 MHz, the duration time of each pulse 15 s, the interval is 60 s and the cycle number is 6. Cells were treated with above different groups of ultrasound followed by incubation at 37 °C for 1.5 h. After that, cell viability was measured *via* MTT method.

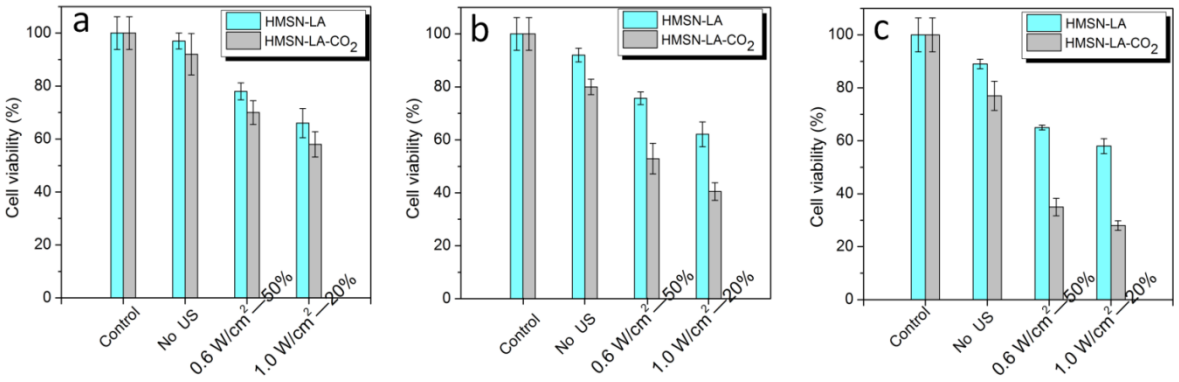

Figure S15 Viability of *in vitro* panc-1 cells treated with different groups *via* MTT method at three concentrations of 0.6 (a), 0.8 (b) and 1.2 mg/ml (c), respectively, wherein control represents no samples, and other three panels represent addition of HMSN-LA and HMSN-LA-CO_2. Other parameters are that ultrasound frequency is 1 MHz, the duration time of each pulse 15 s, the interval is 60 s and the cycle number is 6. Cells were treated with above different groups of ultrasound followed by incubation at 37 °C for 1.5 h. After that, cell viability was measured *via* MTT method.

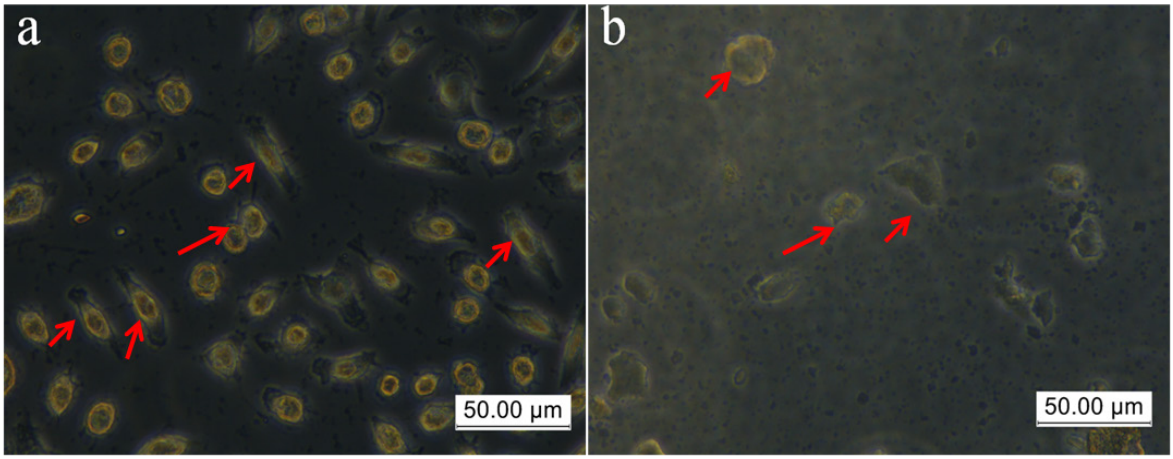

Figure S16 Optical microscopic images of panc-1 cells treated with control group (a) and US+HMSN-LA-CO_2 group (b). US: 1 MHz-1.0W/cm^2-20%-122 KPa, wherein normal adherent cells (indicated by red arrows) can be clearly observed in a, while irregular dead cells can be seen in figure b (indicated by red arrows).

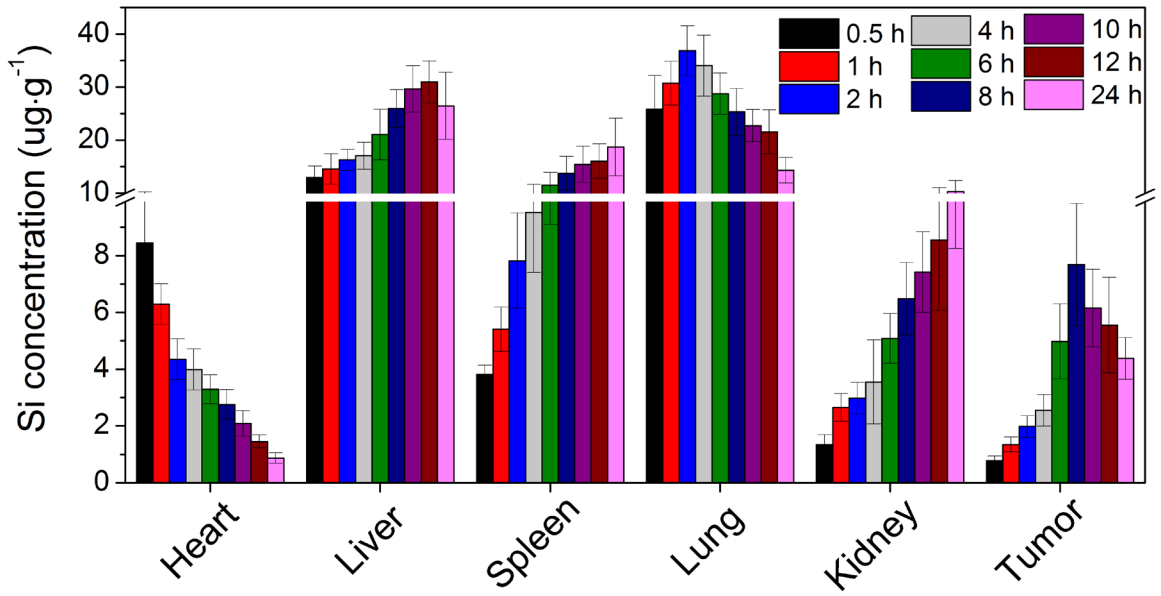

Figure S17 *In vivo* bio-distributions of Si element on behalf of HMSN-LA-CO_2 in different organs of panc-1 tumor-bearing nude mice with expericening different another incubation time after intravenously injecting HMSN-LA-CO_2 *via* ICP method.

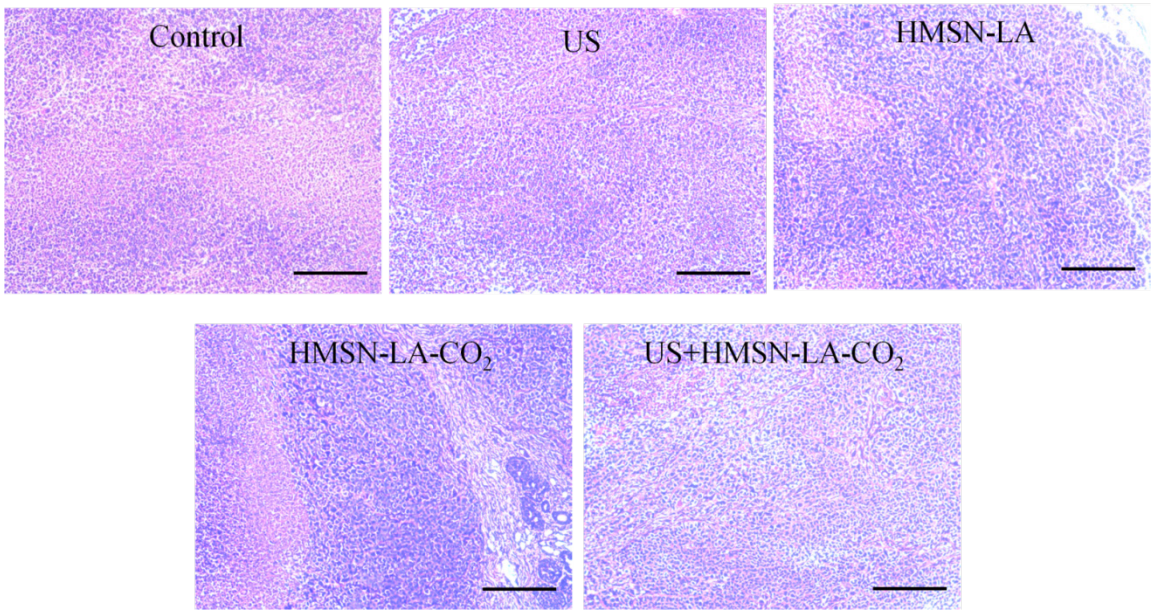

Figure S18 Optical microscopic images of isolated panc-1 pancreatic xenograft solid tumor treated with different groups after H&E staining. The scale bar is 200 um.

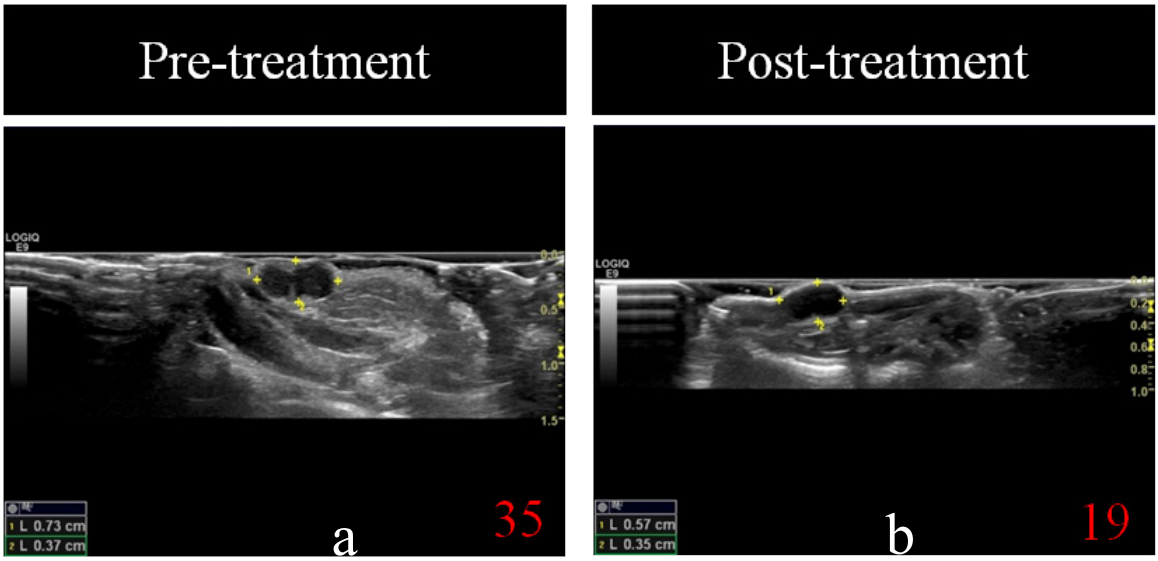

Figure S19 B-mode ultrasound images of panc-1 pancreatic xenograft solid tumor before (a) and after (b) treatment with US+HMSN-LA-CO_2 for 1 day, which can be employed to monitor the variation of tumor volume, and MI=0.6.

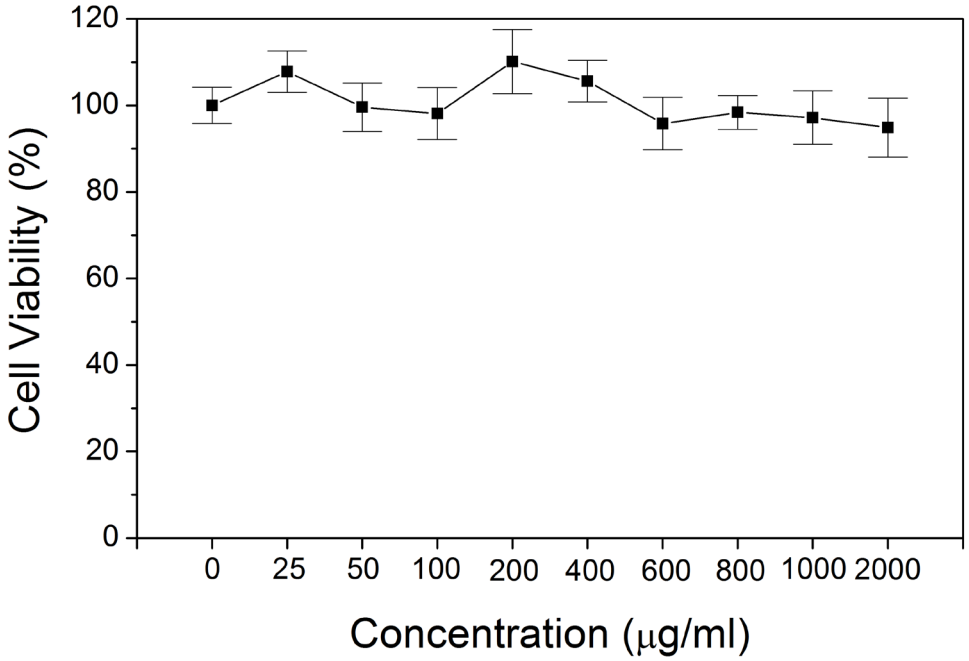

Figure S20 Cytoxicity of L929 after incubation with HMSN-LA of different concentrations for 48 h.

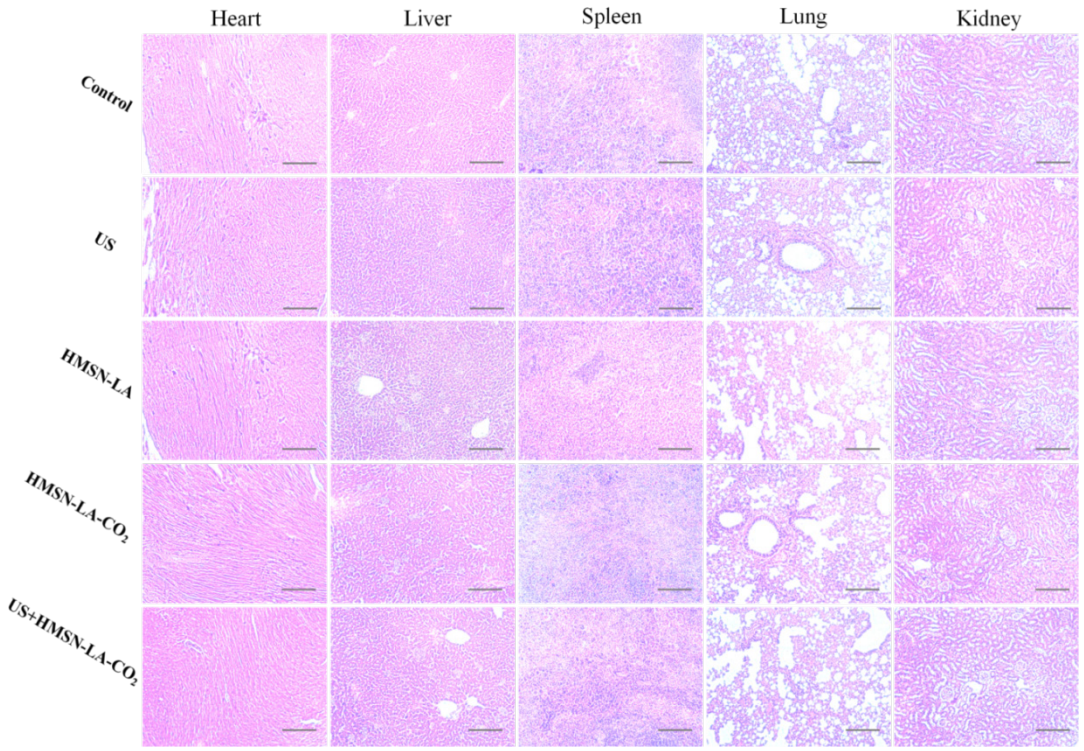

Figure S21 Optical microscopic images of isolated main organs (heart, liver spleen, lung, kidney and tumor) of panc-1 pancreatic tumor-bearing nude mice treated with different groups on the 18th day after H&E staining. The scale bar is 200 um.

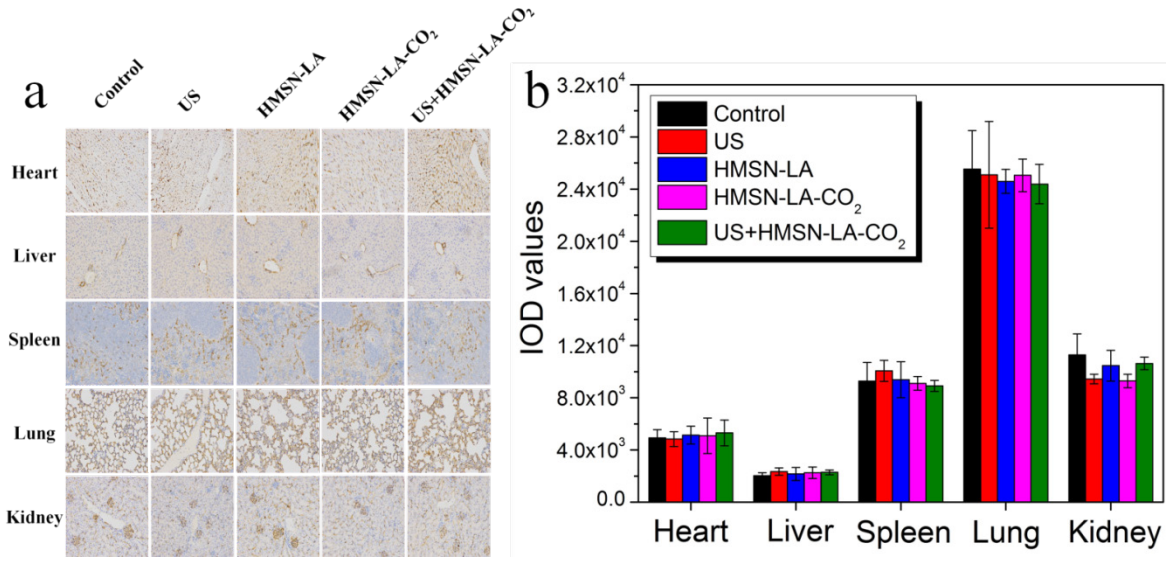

Figure S22 (a,b) Effects of the constructed pH/temperature dual-responsive CO_2 nanobomb system on vessel densities in isolated main organs (heart, liver spleen, lung, kidney and tumor) of panc-1 pancreatic tumor-bearing nude mice, wherein (a) is the optical microscopic images (200-fold) of isolated panc-1 pancreatic xenograft solid tumor treated with different groups after CD34 immumohistochemical staining, and (b) is the quantitative IOD values of the images in (a) determined by Image pro-plus 6.0 sofware. Notes: IOD value is positively proportional to the density of vessels.

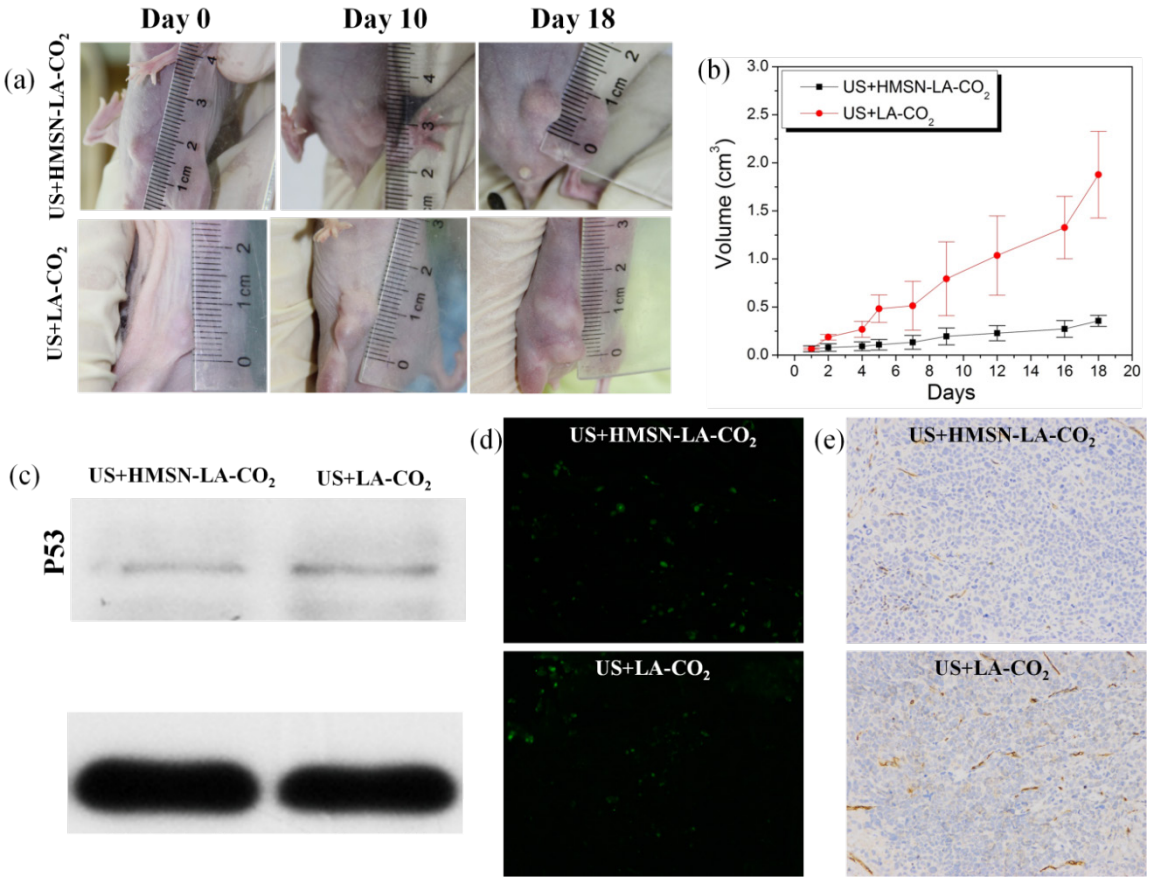

Figure S23 Evaluations and analysis on inhibitory efficiency of panc-1 tumors subcutaneously implanted in nude mice using US+LA-CO_2 and HMSN-LA-CO_2, respetively.(a,b) Volume viriations of panc-1 tumor after treatments with US+LA-CO_2 and HMSN-LA-CO_2 *via* digital recording (a) and voliume measuremt (b). (c,d) Analysis on principles of how US+LA-CO_2 and HMSN-LA-CO_2 to delay gwoth of panc-1 tumors *via* westernblot (c), tunnel (d) and CD34 (e) stainings. In (c,d), there are no differences in P53 expression and apopsotis cells of panc-1 tumors after treatments of US+HMSN-LA-CO_2 and US+LA-CO_2, respectively, indicating neglectable apoptosis, and in (e), the evident difference in vascular density indicates US+LA-CO_2 failed to destroy vasular vessles in panc-1 tumors, demostrating absence of CO_2 bubbles' explosion-induced necrosis (physical damages).